Correlation of Surfactant/Polymer Phase Behavior with Adsorption on Target Surfaces

Joseph O. Carnali* and Pravin Shah

Unilever Research and Development, 40 Merritt Boulevard, Trumbull, Connecticut 06611

Received: February 5, 2008; Revised Manuscript Received: March 18, 2008

In this contribution, the phase behavior of a surfactant/polymer mixed system is related to the adsorption of a complex derived from the mixture onto a target surface. The phase map for the system sodium dodecyl sulfate (SDS, a model anionic surfactant)/pDMDAAC (poly(dimethyl diallyl ammonium chloride), a cationic polymer) shows behavior very typical of surfactant/oppositely charged polyelectrolyte mixtures. The predominant feature is a broad, two-phase region in the phase map which lies asymmetrically around the 1:1 stoichiometry of surfactant charge groups to polymer charge units. The overall controlling principle driving the phase separation is charge compensation. Excess of polymer yields an isotropic solution, as does a great excess of surfactant (termed resolubilization). The phase separating in the SDS/pDMDAAC system is characterized by a positive ζ-potential when the polymer is in excess and a negative ζ-potential when the surfactant is in excess. The surface charge properties of the precipitated phases are essentially identical to those of target particles (ground borosilicate glass) dispersed at the same approximate position in the phase map, suggesting that the surfactant/polymer complex at the precipitation boundary is the same as that adsorbing onto the pigment particle. This conclusion is confirmed by depletion studies which allow the polymer adsorption density to be determined. For polymer-rich systems, essentially all of the surfactant adsorbs along with the polymer via a high-affinity isotherm with a plateau coverage of about 0.8 mg polymer/m^2. Surfactant-rich systems adsorb with a similar affinity, despite the mismatch of the complex charge matching that of the particle surface. Once adsorbed, these complexes are not readily removed by rinsing, though complexes adsorbed from SDS-rich systems will lose excess surfactant upon extreme dilution. Over a wide range of surfactant-rich compositions, from 1:1 stoichiometry out toward the resolubilization zone, a chemical analysis reveals that the surfactant/polymer precipitate species consists of a 1:1 charge complex with the addition of about 0.25 mol of surfactant/mol of complex. Resolubilization of these sparingly soluble species is achieved simply by dilution to below their solubility limit.

Introduction

The general picture emerging from years of study of surfactant/polymer interactions is that their dilute solutions can be characterized in terms of surfactant adsorption on polymer chains as micelle-like clusters. In oppositely charged surfactant/polyelectrolyte systems, complexes of these components show a blending of the phase behavior characteristic of the surfactant alone combined with a strong interaction between the two species. Both the duration of interest in this area and the number of comprehensive reviews available[1–6] are indications of the manifold applications of these kinds of systems in technological areas including personal care products (hair shampoos and conditioners),[7–10] fabric detergents and conditioners, paints and coatings,[11] printing inks, ore floatation, and drilling muds.[12]

Independent variation of oppositely charged surfactant/polyelectrolyte levels produces so-called phase maps[13] which generally show three characteristic regions.[14–19] The most important factor determining the boundaries between these regions is the relative ratio of surfactant-to-polyelectrolyte repeat unit.[20] At low surfactant-to-polymer ratios, where the polymer charge is in excess, the surfactant head groups can bind to the polymer charge sites without significantly reducing the solubility of the resulting complex. This first region of the phase map is thus a transparent, nonbirefringent phase which is termed isotropic. As the surfactant-to-polymer ratio increases, the total charge from the surfactant begins to approach the complimentary charge from the polymer. There is then a tendency for the complex to separate as a liquid-like (coacervate) or solid-like (precipitate)[21] phase in equilibrium with very dilute solution.[22,23] The second characteristic region of the phase map is thus marked by a turbidity or the presence of a definitive second phase. At still higher surfactant-to-polymer ratios, further surfactant association can lead to excess adsorbed species and to resolubilization of the coacervate/precipitate.[24,25] This third region of the phase map is again isotropic.

In the surfactant-poor (polymer-rich) region of the phase map, the association of the polyelectrolyte with surfactant is largely entropy-driven, with the release of the simple monovalent counterions (e.g., Na^+ and Cl^-).[26–32] The elevated local concentration of surfactant around a polyelectrolyte chain leads to the formation of surfactant aggregates (micelles) at total surfactant concentrations well below those typical of the critical micelle concentration (cmc).[33] This cooperative binding using the polymer chain as a template occurs at the critical aggregation concentration (CAC).[34,35] As an example, for the sodium dodecyl sulfate (SDS)/poly)dimethyl diallyl ammonium chloride) (DMDAAC) system as studied in the present report, Lee and Moroi[36,37] determined the SDS CAC to be 1.9×10^{-3} mM at 298 K—the cmc for SDS being about 8 mM[38] under those same conditions. The extent of cooperativity has been shown to depend on several structural parameters including the polymer charge density, the backbone hydrophobicity and flexibility, and

* To whom correspondence should be addressed. E-mail: joseph.carnali@unilever.com. Tel.: 203-381-5444. Fax: 203-381-5487.

10.1021/jp801079v CCC: $40.75
Published on Web 05/21/2008

the alkyl chain length of the surfactant.[12,39–42] Flexible polymer backbones allow the polymer chain to more easily wrap around micelles and allow the chain to adjust, to some extent, the charge density it presents to micelles, making for more facile cooperative binding and a lower CAC.[41,42]

The phase separation region was highlighted in the classic work of Goddard and co-workers,[9,14,15] working with the quaternary ammonium substituted hydroxyethyl cellulose—Polymer JR-400 (Amerchol)—and the anionic surfactant SDS. The key finding was that maximum "precipitation" corresponded to stoichiometric 1:1 surfactant/polymer charge unit neutralization.[33] A general trend found within the phase separation region is that the great majority of the polyelectrolyte is found in the precipitated phase.[16,26] This exaggerated partitioning was found to relax with increasing surfactant concentration as the resolubilization zone was approached.[43] The phase separation region spans some range of surfactant-to-polymer charge unit ratio, depending very much on the parameters of the system under study.[7,21,44,45] Lower limits of about 0.8 were reported by Zhou et al.[19] for cationic hydroxy ethyl cellulose/SDS. Upper limits range widely with 3:1 being reported by Goldraich et al.[20] for Polymer JR/SDS and 10:1 for cationic modified acrylamide/SDS.[12]

The physical form and microstructure of the precipitate phase has been studied in some detail. Macroscopically, the phase was reported to have a gel-like consistency,[16,46] consistent with the dehydration of the surfactant/polyelectrolyte ion pairs. This simple coacervate picture of the separated phase was further refined by Goldraich et al.[20] who used cryo-TEM to study the SDS/Polymer JR-400 system at fixed 0.1% polymer. Microstructures identified as bilayers and vesicles for polymer-rich systems evolved into globular flocs with lamellar packing of surfactants with increasing surfactant level. The appearance of the lamellar packing suggested to the authors that polyelectrolyte binding served to reduce the surfactant headgroup area. The relationship between the mesophases formed by the surfactant/polymer complex and those formed by the surfactant alone provides another way of thinking about the phase separation region. Merta et al.,[22] studying soap/cationic starch systems, determined that the sequence of liquid crystalline phases formed at 1:1 soap/starch stoichiometry varied with increasing soap concentration in the same order and with the same structure as in the case of soap-only systems. Less soap was required with the cationic starch, however, so that the polyelectrolyte counterion was again seen to accelerate the reduction in curvature of the aggregate which would normally have occurred with increasing soap concentration. One viewpoint is that the polyelectrolyte serves to locally concentrate the surfactant and so hasten mesophase formation.[43,47] The above picture is inconsistent with some other observations, however, including those of Svensson and co-workers[44,48] who found that mesophases of higher average interfacial curvature and lower aggregation number (i.e., cubic rather than hexagonal packing) occurred when, for example, polyacrylate replaced bromide as the counterion to cetyl trimethyl ammonium.

The shape and even existence of the resolubilization region is particularly sensitive to the polyelectrolyte charge density and the surfactant structure.[34,42] High polymer charge densities and branched chain or ethylene oxide modified surfactants broaden the phase separation region, necessitating high surfactant-to-polymer levels to reach resolubilization. Resolubilization is generally attributed to association of excess surfactant with polymer beyond charge compensation. Svensson et al.,[44] studying the resolubilization of cationic hydroxy ethyl cellulose with SDS, found that the SDS level at the resolubilization boundary could be expressed as a linear sum of free and polymer-bound surfactant, the latter being the product of the concentration of polymer charge units and the binding ratio of surfactant-to-polymer charge unit. For cationic guars and sodium alkyl sulfates, Anthony et al.[16] found that the bound surfactant per polymer charge exceeded 5 and that there was enough free surfactant for micelles to form. Other estimates for the binding ratio include the 1.5 found by Svensson et al.[44] and the 2.0 found by Zhou et al.,[19] (cationic hydroxy ethyl cellulose in both cases). Light[7] and neutron[24,30] scattering studies are consistent with free surfactant micelles coexisting with micelles bound to polymer chains in the resolubilization region. The interaction of the surfactant/polymer complex with excess surfactant might not occur in the case of high charge density polyelectrolytes, explaining their difficulty in resolubilization. Wang et al.[32] propose that such tight surfactant binding occurs in these cases that the precipitate is dehydrated and cannot be penetrated by excess surfactant.

A less studied aspect of surfactant/polymer interactions is the potential adsorption of the resulting complex to the air/water interface or onto target surfaces. Goddard stated in 1993[4] that a general picture had not emerged connecting the solution behavior (or stoichiometry) of these systems with the nature of the adsorbing species. One reason for this state of affairs is that most adsorption studies have looked at sequential, rather than simultaneous, adsorption of the polymer and surfactant.[49–53] Arnold and Breuer[54] studied adsorption from the SDS/Polymer JR-400 system on finely divided γ-alumina and postulated that SDS acted to bridge the cationic polymer to the cationic substrate, with the surfactant/polymer ratio in the adsorbed layer differing from what was found in the bulk. Dedinaite and co-workers[17,55] exposed mica to complexes between SDS and poly(2-(propionyloxy) ethyl trimethyl ammonium chloride). In the bulk, peak turbidity was observed at a 3:1 surfactant/polymer charge ratio, but the ζ-potential of mica surfaces exposed to this bulk solution was essentially zero. The result suggested that a 1:1 stoichiometric complex was adsorbing, perhaps with SDS leaving the bulk complex via ion exchange with the anionic surface. Evidence showing some correlation between solution and adsorbed layer structure comes from an atomic force microscopy (AFM) study of adsorbed SDS/Polymer JR-400 complexes by Zimin et al.[18] These authors determined that the adsorbed layer structure was independent of the substrate, implying that the state of the complex in solution/dispersion controlled the morphology of the deposit. Additionally, Chen[12] observed that reversal of the ζ-potential of silicone—oil emulsion droplets and their peak flocculation coincided with surfactant/polymer ratios giving maximum turbidity in the bulk.

When there is a strong electrostatic component to the adsorption, binding is generally found to be irreversible. It is generally understood that surfactant/polymer complex binding to a surface is driven by the translational entropy gain due to the release of the small counterions to the surface. Upon rinsing and dilution of the ionic strength, the entropy gain actually increases, strengthening the binding.[17,43,56] Another point of view attributes the insensitivity to dilution to the insolubility of the stoichiometric complex.[26] Other workers have suggested that the state of the adsorbed layer and its durability depend on the order of addition. It is generally found that a cationic polymer alone, once adsorbed to a negative oxide surface, cannot be removed by rinsing with either dilute electrolyte or anionic surfactant solution.[49] Preadsorbed surfactant/polymer complexes,

on the other hand, can be partially depleted of surfactant by rinsing with dilute electrolyte.[55,57]

Despite the considerable activity reviewed above, there remain some aspects of surfactant/polymer interactions which still require clarification. As an example, the entire third region of the generalized phase map, the resolubilization zone, is less studied than the other two regions and less understood. In particular, the situation with highly charged polyelectrolytes is complicated by the fact the resolubilization zone with an oppositely charged surfactant is often unattainable. For cost and performance reasons, the polymer levels employed in most applications of these systems lead to surfactant-rich stoichiometries. Where resolubilization does not occur, these applications are often dominated by a separate precipitate phase. The surfactant-to-polymer ratio can exceed 100 in some of these cases. In the present study, an anionic surfactant/cationic polyelectrolyte system is considered which is rather typical of those employed commercially. The system SDS/pDMDAAC represents just such a high charge density situation as discussed above, in which the phase separation region is rather extensive and resolubilization is difficult. The phase map of this system is considered in detail with emphasis on the phase separation and resolubilization regions. The electrophoretic properties of precipitate phases are shown to be controlled by the total ratio of SDS to pDMDAAC, and this pattern is maintained in the isotropic regions where the surfactant/polymer complex conveys the same properties to a target surface. Depletion studies prove that those complexes adsorb without change of composition and are largely resistant to being rinsed off. The phase-separated species is characterized chemically over a wide portion of the phase map, and the dominance of the charge stoichiometric surfactant/polymer complex is demonstrated. Lastly, a mechanism for resolubilization of this complex is proposed.

Experimental Section

Materials. The polymer studied was a commercial sample of Merquat 100 obtained as a gift from Nalco Corporation as a nominal 40% solution. This solution was diluted 2-fold with water (all water was treated with a Barnstead E-Pure water purification system to give type 1 reagent grade water with a resistivity of 18.2 MΩ·cm) and then filtered through a 10 μm mesh to remove any gross insolubles. The filtrate solution was then dialyzed for 3 days against water, using a 3500 molecular weight cutoff membrane (Spectra/Por 3),[58,59] with the phase external to the dialysate being exchanged twice daily. The recovered polymer solution was stored in a refrigerator until needed. The polymer content was determined by thoroughly dehydrating a portion of the sample, first by oven-drying at 45 °C and then by evacuation over P_2O_5, the later step being necessary as the polymer was found to be hydroscopic. A parallel solution, prepared using a 12−14 000 molecular weight cutoff membrane in the dialysis, yielded results which were indistinguishable from the above. Merquat 100 is a homopolymer of dimethyl dially ammonium chloride (pDMDAAC). The molecular weight of a different batch of this material was previously determined as 200 000 by the gel permeation chromatography (GPC) technique.[60] The theoretical charge density of pDMDAAC, based on the molecular formula, is 6.2 meq/g, but measurements by colloidal titration using toluidine blue as indicator and potassium polyvinyl sulfate as titrant indicate a lower value of 5.2 meq/g.[37] The charge density of the polymer used in this study was determined as 5.8 ± 0.2 meq/g by elemental analysis for nitrogen by Schwarzkopf Microanalytical Laboratory, Inc. (Woodside, NY). SDS was obtained as a sample of OmniPur grade from EMD Chemicals. This material had a purity stated by the supplier as 99% and was further recrystallized twice from absolute ethanol.

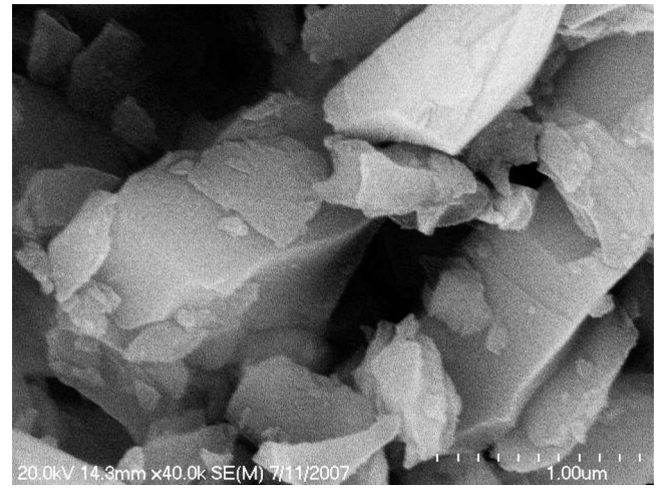

Figure 1. Electronmicrograph of the glass powder sample showing angular particles with a noticeable small particle tail but no obvious porosity. The scale bar at the bottom-right represents 1.0 μm.

The glass powder was a sample of Duran borosilicate glass provided by Schott Glass North America as glass no. 8330. This material had a density of 2.23 g/cm^3, and it size distribution was characterized by the supplier as $d_{50} = 1.06$ μm and $d_{99} = 2.90$ μm. An electronmicrograph of the powder (Figure 1) shows it to consist of nonporous, angular particles with a particle size distribution which clearly tails into the submicrometer range—explaining the high particle surface area of 15 ± 0.5 m^2/g (BET method, Micromeritics Analytical Services, NC). This powder was supplied at high purity and was treated by dialysis against 3 mM sulfuric acid using 3500 molecular weight cutoff dialysis tubing (Spectra/Pore 3). Dialysis was continued for 2 days with periodic replacement of the acidic external phase, after which water was substituted and the dialysis continued until the external phase pH held steady at 5.5 (the starting pH of the purified water). The glass was then dried down to a powder and stored in a desiccator until use. The point-of-zero-charge (p.z.c.) of this glass powder was determined as 3.0 ± 0.5 by microelectrophoresis at a background electrolyte level of 0.01 M NaCl (see Figure 2 and the discussion below). This value is in good agreement with published values.[61] It will be of subsequent interest to note that the ζ-potential of the glass powder in the pH range of 5−6 used in this study is approximately −60 ± 5 mV.

Methods. ***Phase Studies.*** Separate stock solutions of pDMDAAC and SDS were prepared in a background ionic strength of 0.01 M NaCl. This background ionic strength yields a Debye length of 3 nm (or less) for all of the systems (less in the case of high surfactant concentration). A phase map was constructed by choosing initial polymer or surfactant solutions as further dilutions from the stocks (all dilutions being made with 0.01 M NaCl) and then delivering appropriate weights of each solution into glass tubes equipped with screw top lids. The total weight of each sample was kept constant at 5.0 g so that the path in composition space spanned by a single series (combinations of one stock polymer dilution and one stock surfactant dilution) is an arc as indicated in Figure 3. The tubes were sealed and then agitated by successively inverting the tubes many times. Agitation was performed several times everyday for several days to ensure complete mixing. The sets of tubes were stored either at room temperature (23 °C) or at 50 °C in a temperature-

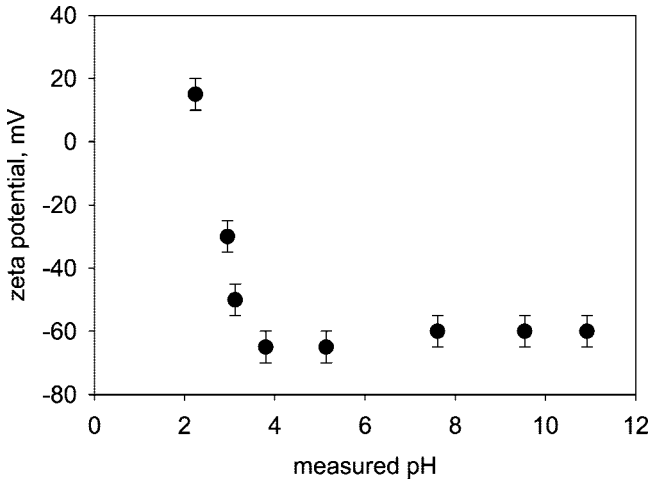

Figure 2. Electrophoretic behavior of the glass powder at a particle level of 0.02% in 0.01 M NaCl as a function of pH. The point-of-zero-charge (p.z.c.) can be estimated as 3.0 ± 0.5.

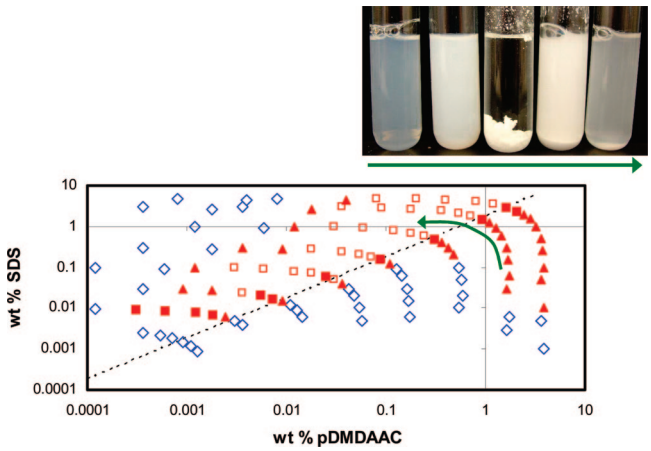

Figure 3. Phase map for the SDS/pDMDAAC system, showing the two-phase region at 23 °C and at a background ionic strength of 0.01 M NaCl. Data points indicate individually constructed samples whose appearance is indicated by the appropriate symbol: open diamonds, isotropic; closed triangles, Tyndall scattering; solid squares, clear supernatant and solid sediment; open squares, solid suspension. The dotted line connotes 1:1 charge stoichiometry between the polymer DMDAAC subunits and the SDS. The inset shows the appearance of selected samples from the two-phase region. Arrows indicate the progression of the samples around the selected arc.

controlled oven. In practice, all systems reached their final appearance within a few hours of mixing and were then invariant over the entire course of the study (~6 months). The phase behavior was observed by viewing the tubes under bright, indirect light and by viewing in transmitted light while the tube was between crossed sheets of polarized film. No difference in the phase behavior was observed between room temperature and 50 °C.

Selected compositions showing a sedimented solid phase were scaled up to 25 or 50 g in plastic centrifuge tubes and allowed to equilibrate at room temperature for several weeks. The supernatant phase isolated by centrifugation was completely clear and was transferred to a pretared weighing bottle. The sedimented phase was washed with a minimal amount of ice-cold water and then placed in a pretared cup. In all the cases reported, the separation and collection of the two phases (precipitate and supernatant) was judged to be semiquantitative, with losses of material never exceeding 3%, as judged by mass balance. Both phases were dried down completely. The supernatant was first dried in a 45 °C oven to remove all obvious water, then stored several days in a desiccator over Drierite, and finally dried under vacuum over P_2O_5. In this way, a percent solids could be calculated for the supernatant. The precipitated phase was not treated in the oven but was otherwise dried in the same way as the supernatant. In order to obtain a water content for the precipitate, the dried solid was re-equilibrated over a saturated solution of $BaCl_2$ (92% RH) until a constant weight was achieved. This level of water activity was chosen to avoid the complication of capillary condensation.[62] All of the dried phases were analyzed for nitrogen and sulfur by Schwarzkopf Microanalytical Laboratory.

Electrophoretic Characterization. The ζ-potential of a surface is the electrical potential measured very near that surface—at the so-called "plane of shear". This plane occurs at the boundary between the stagnant solvent layer which travels with a dispersed particle and the surrounding solution. The ζ-potentials of glass powder particle dispersions in surfactant/polymer solutions and of incipient precipitates in surfactant/polymer solutions were measured using the model 501 Lazer Zee meter (Pen Kem, Inc.). This device is a standard microelectrophoresis instrument and works by illuminating the sample with a laser and then viewing the light scattered at 90° through an optical microscope. Particles with sizes in the range of 0.2−10 μm can be viewed as distinct scattering centers. The electrophoretic mobility, U, is defined as the ratio of the electrophoretic velocity of the particle to the applied electric field strength. The mobility is then related to the ζ-potential via the following equation:

$$U = C(\varepsilon_0 \varepsilon_r \zeta/\eta) \quad (1)$$

where ε_0 and ε_r are the permittivity of free space and the relative permittivity, respectively, and η is the viscosity of the suspending medium. C is a constant for a fixed particle size and solvent composition and has a magnitude near unity. In the present study, the ionic strength was kept nearly constant by the background 0.01 M NaCl electrolyte and the same batch of particles was used throughout. The Debye length for this background electrolyte level (the reciprocal Debye length is defined as $\kappa = [(1000e^2N_A/\varepsilon_0\varepsilon_r kT)\sum z_i^2 M_i\ ]^{1/2}$, where e is the elemental charge, N_A is Avogadro's number, and z is the valency of the electrolyte at molarity M) is 3.03 nm.[63] Such conditions correspond to the product κR (where R is the particle size) being large so that C can be taken as unity (Smoluchowski equation).[64,65] On the basis of measurement of a titanium dioxide standard colloid (Laszlo I. Kovacs Consulting), the accuracy of the data can be estimated at ±2.5 mV.

The procedure typically employed in the measurements depended on whether the glass powder particles or incipient precipitates were being observed. In the particle case, a surfactant/polymer system was chosen whose composition put it in an isotropic region of the phase map. An aliquot of a glass powder dispersion in 0.01 M NaCl was then added to the surfactant/polymer solution to give a final particle level of 0.02%. All such dispersions were made in plastic labware to eliminate any loss of polymer due to adsorption to the labware surface. The dilute slurry was placed in an ultrasonic bath (Fisher model FS140) for 10 min to fully disperse the particles. This slurry was then transferred to the microelectrophoresis cell for measurement. The effect of varying the sonication time, as well as the total time of particle exposure to the solution, was explored and it was found that the above procedure was sufficient to obtain equilibrium results. As an aside, this finding strongly suggested that the adsorption kinetics under these conditions are relatively rapid.

In the case of the incipient precipitates, samples were chosen from the polymer/surfactant phase map which showed a low level of Tyndall color but no visible precipitate (see below). These samples were added directly to the electrophoresis cell where it was observed that the Tyndall scattering could be related to scattering centers whose mobility could be followed as for the particles. The number density of these centers increased with the level of Tyndall color. As long as this number density was low enough for distinct scattering centers to be observed, measurement was straightforward and no dependence of the measured ζ on the strength of Tyndall scattering was detected.

For measurements on bare glass powder particles, the reported values of ζ should closely approximate the true ζ-potential. For the incipient precipitates and for the particles exposed to surfactant/polymer solutions, on the other hand, uncertainties can arise in terms of the location of the plane of shear. In these cases, it is more prudent to interpret the reported ζ-potentials as representing the underlying electrophoretic mobility.

Adsorption Isotherms. Adsorption from surfactant/polymer systems onto glass powder particles was determined using the depletion method. Glass powder was preweighed into plastic centrifuge tubes equipped with screw caps. A small magnetic stir bar was added, and the powder was vigorously stirred as a surfactant/polymer system from the surfactant-rich or polymer-rich single-phase region was added. The centrifuge tube was then immediately transferred to an ultrasonic bath where it was treated for 10 min, followed by end-over-end tumbling for 24 h. This procedure was judged as an effective means of rapidly exposing all of the available glass surface to the surfactant/polymer system, while allowing ample time for adsorption equilibrium. The supernatant was the then isolated by centrifugation at 3000 rpm for 15 min. The residual carbon and nitrogen in the supernatant was determined by the New Hampshire Water Resources Research Center (University of New Hampshire, Durham, NH 03824) via high-temperature catalytic oxidation (HTCO) using a Shimadzu TOCV equipped with a TNM nitrogen detector. The sample is combusted on a heated catalyst (720 °C) and the resulting products, CO_2 and N_2O, are measured with a nondispersive infrared detector (NDIR) and a chemiluminescence detector, respectively. The accuracy of the measurements was determined as $\pm 5\%$ for both carbon and nitrogen across the concentration ranges investigated. After conversion to the equivalent residual masses of surfactant and polymer, the adsorbed amount was calculated as the difference with respect to the concentration prior to exposure to glass. In a traditional adsorption experiment, the concentration of adsorbate is varied at fixed adsorbent. In this study, the exact same adsorbate solution, a single point on the phase map of Figure 3, was used for a particular isotherm in order to guarantee the same adsorbing species. The weight of glass powder was varied over a series of samples to create a range of target surface area and corresponding variation in measured depletion.

Results

Phase Map. The results for the SDS/pDMDAAC system are shown in Figure 3. The data points correspond to a series of arcs, each of which represents the mixing of a single polymer solution with a single surfactant solution in differing proportions. A defining characteristic of each arc is that the systems are isotropic when either the polymer or the surfactant level is very low (indicated by the open diamond symbols). The series based on blending 1.8% pDMDAAC and 3% SDS (second arc from the top of Figure 3) gives a good overall indication of the results. With the polymer level at 1.8% and the SDS level below about 0.03%, the systems are isotropic. As the surfactant fraction increases (moving counterclockwise around the arc, as indicated in Figure 3), the samples first start to show a faint Tyndall color (filled triangle symbols), suggesting the occurrence of a second phase on the colloidal size range. The intensity of the Tyndall scatting increases steadily as the surfactant fraction increases, until the samples become essentially opaque by 1% SDS. This trend can be seen in the inset to Figure 3, which shows, left to right, the actual sample tubes for increasing surfactant/polymer ratio counterclockwise around the apex of the arc. Higher SDS fractions at first lead to the appearance of a macroscopic precipitate and clear supernatant as indicated in the figure inset and by the solid square symbol in the phase map. The amount of precipitate in this sample is the highest to be found anywhere along this particular arc, and the white rubbery nature of the solid is rather singular as well. The two phases occurring at still higher SDS fraction consist of a more finely dispersed precipitate which settles very slowly from a supernatant which retains some turbidity—indicated by open square symbols in the phase map. This residual turbidity decreases, as does the amount of precipitate, as the SDS level exceeds about 2%, until ultimately the system clears entirely (solid triangles = Tyndall blue through to isotropic = open diamonds).

As a guide to interpreting Figure 3, a dotted line has been inserted which indicates the condition for 1:1 charge stoichiometry between the pDMDAAC (with a repeat-unit molecular weight of 161.7) and the SDS (with a molecular weight of 288). The line corresponds to an SDS-to-polymer weight ratio of 1.7. For the 1.8% pDMDAAC arc, this line passes through the singular system of maximum macroscopic precipitate and transparent bulk phase—the middle test tube of the inset to Figure 3. In general, for the other arcs in the phase map, the stoichiometric line passes through the midpoint of the arcs and the points of maximum macroscopic precipitation (indicated by solid squares). However, the stoichiometric line appears to fall under the precipitation region for the most diluted arcs—indicating the finite strength of the complex binding. The two-phase region is distributed asymmetrically about the 1:1 line. Except for the highest polymer levels, the polymer-rich isotropic region extends up to the vicinity of the stoichiometric line. However, the other edge of the two-phase region does not occur until the system is very much enriched in SDS.

The reversibility of the phase behavior was investigated by allowing samples from each of the surfactant-rich and polymer-rich isotropic phases and from within the phase separation region to equilibrate for several days. Then the individual systems were mixed with excess surfactant or polymer or diluted so as to move the composition into a different region of the phase map. The samples were found to re-equilibrate to the same phase behavior as observed when the identical composition was prepared directly. The one exception was the 1:1 stoichiometic system of maximum precipitation and clear supernatant. The rubbery sediments in these systems were not observed to re-equilibrate during these studies. Reversibility was particularly obvious in the isotropic region at low surfactant/polymer ratio where freshly prepared samples frequently contained a precipitate. These sediments presumably occurred due to the presence of high local SDS levels as small volumes of surfactant solution were added to bulk polymer solution. Within a hour, however, the precipitate redissolved and the system became isotropic.

Electrophoretic Characterization of Precipitates. As a step in characterizing the nature of the surfactant/pDMDAAC association, systems from the surfactant-rich and polymer-rich

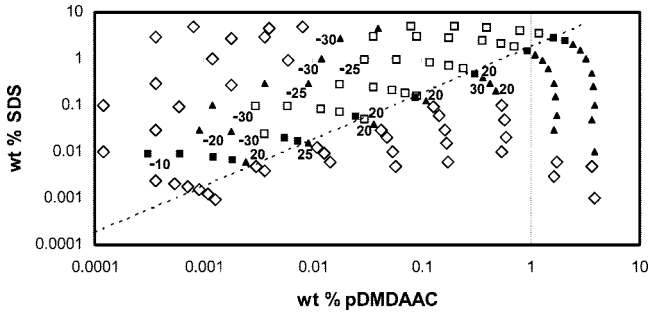

Figure 4. Measured ζ-potential of the incipient precipitated phase at the indicated points in the SDS/pDMDAAC phase map. Symbols have the same meaning as in Figure 3.

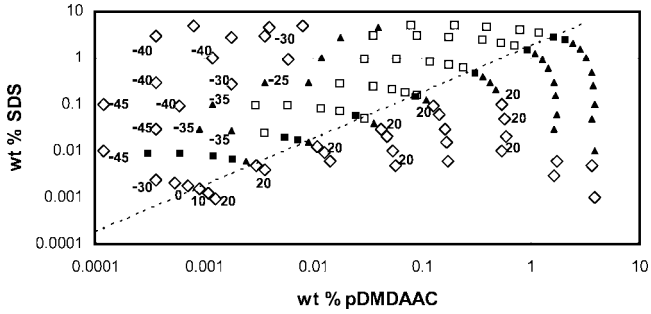

Figure 5. Measured ζ-potential of glass powder particles (at a level of 0.02%) dispersed at the indicated points in the SDS/pDMDAAC phase map. Symbols have the same meaning as in Figure 3.

edges of the phase separation region identified in Figure 3 were studied for their electrophoretic properties. Samples just inside the two-phase region, which typically showed Tyndall color, were analyzed, and the measured ζ-potential is reported in Figure 4, with the measured value superimposed on the relevant location in the phase map. It is observed that the precipitation which is incipient toward the polymer-rich edge has a positive surface charge, showing a ζ-potential of about +20 mV. The ζ-potentials measured on the incipients from the surfactant-rich edge show the opposite sign with a value of −20 to −30 mV.

Moving just across the phase boundary edges, into the isotropic regions of the phase map, the samples lack any observable scattering centers and cannot be analyzed. However, by adding a dilute dispersion of glass particles, a surface is present onto which polymer, surfactant, or polymer/surfactant complexes can adsorb. Such adsorption can be detected by following any changes in the ζ-potential of the particles.[66,67] The measured ζ-potentials are reported in Figure 5, with the measured value again superimposed on the relevant location in the phase map. The reported ζ-potentials were found to be quite reproducible over repeated independent determinations. By way of reference, the natural ζ-potential of the bare glass powder particles under the pH and ionic strength conditions employed is −60 ± 5 mV (see Figure 2). As was the case with the incipient precipitates in Figure 4, the measured ζ-potentials in Figure 5 indicate a positive surface charge, again with ζ of about +20 mV, just to the isotropic side of the polymer-rich edge of the phase separation region. As the particles are anionic to begin with, the observed surface charge would appear to be controlled by the absorption of a species derived from the cationic polymer. Although the locations on the phase map studied in Figures 4 and 5 differ somewhat, with those in Figure 5 having a lower surfactant/polymer ratio than the corresponding location in Figure 4, it is still noteworthy that the adsorbing species is so similar, surface potentialwise, to the adjacent incipient precipitate. Just outside the surfactant-rich edge of the phase separation region, the particles have a distinctly negative surface charge which decreases from a measured ζ of about −30 mV adjacent to the phase boundary to about −45 mV at the lowest studied polymer concentrations. As the incipient precipitates showed a ζ-potential of −20 to −30 mV at the relevant phase boundary, it is again tempting to suggest that a closely related species is adsorbing onto the glass powder particles. The trend toward more negative ζ-potential with increasing surfactant/polymer ratio could represent a change in the adsorbing species or in the location of the plane of shear around the particles. Pursuing the former explanation, it would seem reasonable to propose that the stoichiometry of the adsorbing complex would become richer in surfactant and poorer in polymer upon moving from the surfactant-rich edge of the phase boundary in the direction of higher surfactant/polymer ratio. It would then follow that the surface charge of the adsorbing complex should become more negative, and also the resulting ζ-potential of the particles. An alternative possibility is that the total mass of polymer decreases on moving as indicated above so that the number of complexes available for adsorption declines. At a fixed glass loading, the particle ζ-potential could then be expected to trend more negative simply due to exhaustion of the adsorbing species. The glass particles would then be expected to be less affected by the complex species and to follow their own natural tendency toward a more negative ζ-potential. However, this alternative explanation was disproved by varying the glass powder level at fixed SDS/polymer composition and observing that the ζ-potential was invariant for a range of low glass levels. This finding suggests that the surfactant-to-polymer ratio of the complex becomes more surfactant-rich upon moving counterclockwise away from the phase boundary edge in Figure 5.

The arc in the phase map based on 0.002% pDMDAAC and 0.05% SDS (lowermost arc in Figures 3–5) is dilute enough that a phase separation region is not apparent and the ζ-potential of suspended glass powder can be followed throughout its entire course. The results shown in Figure 5 are that the particles clearly pass from a positive surface charge on the polymer-rich side to a negative surface charge on the surfactant-rich side of the arc, through a zone a zero surface charge in the vicinity of the 1:1 stoichiometric line. By the implications drawn above, the species adsorbing on to the particles would be expected to show the same trend in surface charge. A similar result has been reported by Goddard and Hannan[14] for the system of Polymer JR-400/SDS and by Dedinaite and Claesson[17] for poly(2-(propionyloxy) ethyl) trimethylammonium chloride/SDS, where in both cases the SDS level was varied at constant polymer.

Assuming that the measured ζ-potentials of the glass powder indicated in Figure 5 are controlled by the adsorbed surfactant/polymer complex, the behavior of the adsorbed species upon dilution can also be studied by the electrophoretic approach. Glass suspensions at 0.01% solids were prepared in isotropic systems on several of the arcs in Figure 5, selected to the polymer-rich or surfactant-rich side of the biphasic region. The suspensions were loaded into plastic centrifuge tubes and spun at 3000 rpm for 10 min to isolate the particles. All but 2 mL of the supernatant was discarded, and the sediment was resuspended in 0.01 M NaCl for a dilution factor of approximately 1 to 15. The suspension was treated in the ultrasonic bath for 10 min to ensure redispersion of the particles, whose ζ-potential was then remeasured. The dilution process was then repeated for a total dilution of approximately 1 to 225. Results for samples running down the polymer-rich phase boundary, along with their first and second dilutions, are shown as the upper set

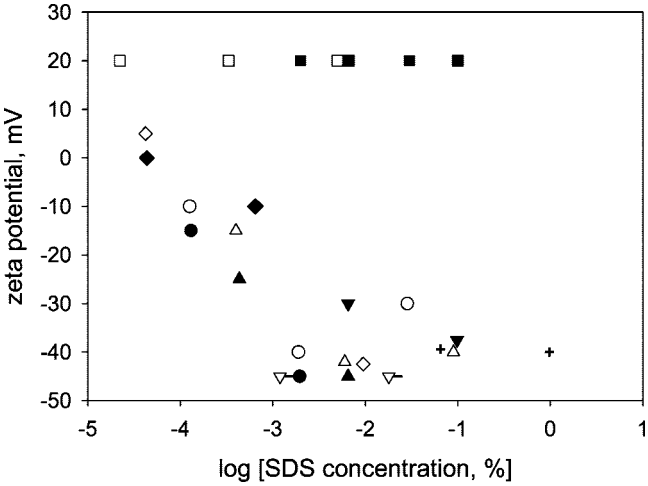

Figure 6. Measured ζ-potential of dispersed glass powder in the SDS/pDMDAAC system diluted along the polymer-rich (upper curve, square symbols) or polymer-poor (lower curve) edges of the two-phase region. Common symbols refer to a particular suspension system and its dilution(s). The extent of dilution is indicated by the corresponding SDS concentration.

of symbols in Figure 6 with positive ζ-potentials. Common symbols indicate a particular suspension and its dilution(s). The abscissa in the plot is the appropriate SDS concentration of the suspension, accounting for any dilution. A similar representation can be made using the polymer concentration to keep track of the dilution. Results for samples running down the surfactant-rich edge of the two-phase region are similarly shown by the lower set of symbols in Figure 6 where the ζ-potential is generally negative.

Along the polymer-rich edge of the boundary, it is observed that dilution does not affect the ζ-potential of the particles, implying that the complex adsorbed from the polymer-rich domain is not influenced by dilution. Along the surfactant-rich edge of the boundary, two effects can be noted. At low dilution, there is a variation in the reported ζ-potential which is attributable to the SDS/polymer ratio of the undiluted sample, as explained above. However, the particle ζ-potential of a particular system is unaffected by the dilution, as described previously. Upon higher dilution, it is observed that the ζ-potential of the resuspended particles moves in a positive direction relative to the undiluted systems, ultimately reaching a state of essentially zero charge. These results suggest that the complex remains adsorbed to the glass during dilution (otherwise the ζ-potential would tend toward that of the native glass, −60 mV). However, the complex appears to undergo some loss of excess anionic surfactant during dilution and tends back toward the stoichiometric 1:1 association.

Adsorption of Polymer-Rich and Polymer-Poor Complexes. Adsorption isotherms measured by depletion provide a more unequivocal picture of the state of surfaces exposed to these types of surfactant/polymer complexes. On the polymer-rich side, an isotropic system was constructed by mixing 0.006% pDMDAAC and 0.01% SDS, corresponding to the first data point on the polymer-rich side of the second arc from the bottom of Figure 3. The adsorbed nitrogen (from the pDMDAAC) is shown in Figure 7a plotted versus the residual nitrogen in the supernatant. In this plot the level of glass powder decreases on going from left to right along the abscissa. Clearly, the polymer is completely depleted at the highest levels of glass employed, and the isotherm is of a high-affinity type with the rapid development of a plateau over the range of 0.2−1.5 ppm residual

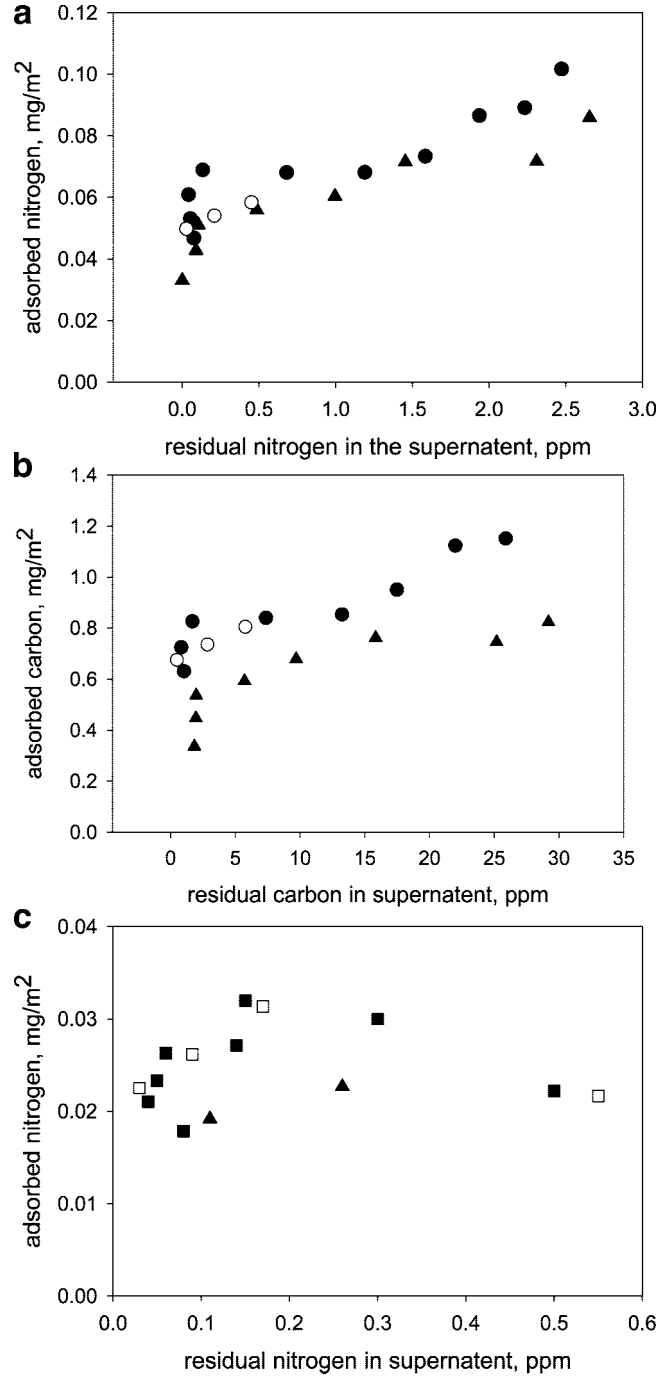

Figure 7. (a) Adsorption isotherm for nitrogen (from pDMDAAC) measured by depletion from the isotropic solution corresponding to the right-most data point of the second arc from the bottom of Figure 3. The level of adsorbent glass powder increases from right to left along the abscissa. Different symbols apply to independent trials. (b) Adsorption isotherm for carbon (contributed by pDMDAAC and SDS) measured by depletion as in (a). (c) Adsorption isotherm for nitrogen (contributed by pDMDAAC) measured by depletion from the solution corresponding to the first isotropic system to the left of the 1:1 stoichiometric line on the fourth arc of Figure 3. Different symbols refer to independent trials.

nitrogen. This plateau corresponds to the equivalent of 0.8 ± 0.05 mg of pDMDAAC adsorbed/m^2 of glass surface. The situation regarding carbon is shown in Figure 7b, where the depleted carbon has been independently determined from the same supernatant solutions as in Figure 7a. The adsorbed carbon (now from both the pDMDAAC and the SDS) is shown plotted versus the residual carbon. The scatter in the carbon

data from independent trials is a little higher than with the nitrogen data, but it is apparent that depletion is again complete at the highest levels of glass. This finding immediately suggests that essentially all of the SDS in this polymer-rich system is associated with the polymer and that the composite species adsorbs with high affinity to the glass surface.

On the surfactant-rich side, a system was constructed by mixing 0.18% pDMDAAC and 0.3% SDS, corresponding to the first isotropic point to the left of the 1:1 stoichiometric line on the fourth arc from the top of Figure 3. From its location on the phase map, it is apparent that the polymer level of this system is relatively low and the SDS level is relatively high. In practical terms, this observation means that it will not be possible to measure the depleted carbon, as the SDS makes a dominating contribution to the total carbon in the system. The low polymer level likewise limits the accuracy to which nitrogen adsorption can be measured by depletion. Trials were conducted with the third arc from the top in Figure 3, but relatively large levels of glass would have been required and difficulties were experienced in reproducibly dispersing such large masses of glass. As a result, the range of depletion which could be explored on the surfactant-rich side was limited. Reasonable data were obtained, however, over two independent trials as shown in the adsorption isotherm of Figure 7c. This isotherm is again of the high-affinity type. From the nitrogen lost in depletion, an adsorption density of 0.3 ± 0.05 mg/m^2 can be determined, interpreted solely in terms of the pDMDAAC. As will be discussed below, there will also be a contribution from the coadsorbed SDS.

Analysis of Separated Phases. As noted above, samples from the apex of the upper arcs in Figure 3 contained an obvious solid phase which was isolated so that chemical analysis could be preformed on both the precipitate and the supernatant. The arcs based on 1.8% and 4% pDMDAAC yielded such samples, at and to the surfactant-rich side of 1:1 stoichiometry. The analysis reported in Figure 8 shows the concentration of surfactant in the supernatant phase (by elemental analysis of the solids isolated from the supernatant for sulfur) as a function of the total surfactant-to-polymer weight ratio. As shown in Figure 8b, the supernatant is essentially devoid of surfactant at an SDS-to-polymer ratio of about 1.60, close to the 1.7 ratio predicted for stoichiometric charge compensation. At higher total surfactant-to-polymer ratio, the surfactant concentration in the supernatant increases with the ratio, approximately linearly at first and then approaching a plateau (Figure 8a). The trend for both the 1.8% and 4% pDMDAAC arcs is the same, whereas the plateau varies due to the different SDS level of the two arcs. A possible interpretation of these results is that, to a first approximation, the surfactant is essentially all bound to the polymer at this total ratio of 1.6 and results in precipitation of a 1:1 complex. At higher total ratios, the "excess" surfactant remains unassociated with the precipitated phase, residing instead in the supernatant. The water content of the precipitated phases was estimated by rehydration at 92% RH (see above). A consistent water level of $16\% \pm 1\%$ was observed for all the samples studied. By comparison, precipitated 1:1 complexes of SDS with poly(ethylenimine) were found to have no strongly bound water.[68]

The above qualitative picture of surfactant distribution between the phases can be further refined by determining the level of surfactant actually in the precipitate. This level is expressed as the number of moles of surfactant associated per mole of 1:1 complex—each complex assumed to consist of a surfactant associated with an oppositely charged polymer repeat unit. In this expression, the surfactant and polymer levels were

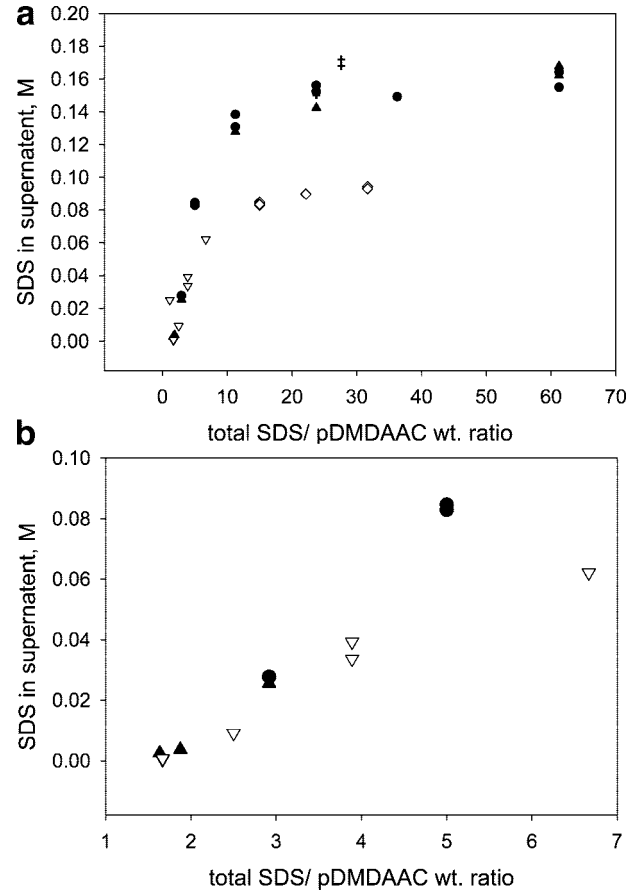

Figure 8. (a) Concentration of SDS in the supernatant phase as a function of the total surfactant-to-polymer weight ratio for selected samples from the top two arcs in Figure 3. Upper solid symbols correspond to the uppermost arc (constructed from 4% pDMDAAC) and lower open symbols correspond to the second arc (constructed from 1.8% pDMDAAC). Panel b is an enlargement showing the behavior at low SDS levels.

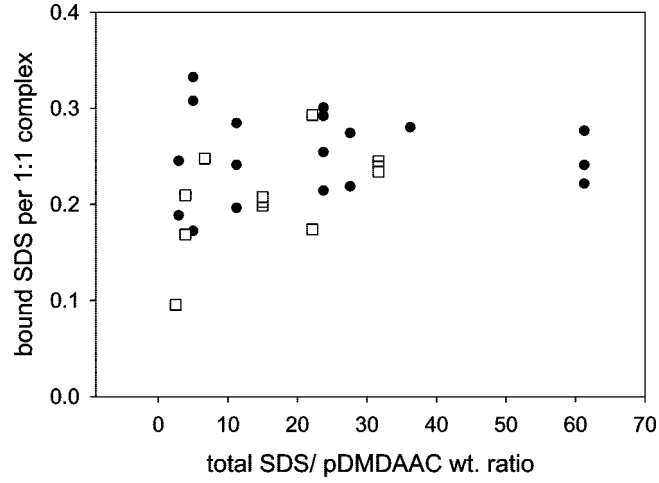

Figure 9. SDS found in the precipitate phase, interpreted as moles bound per mole of 1:1 SDS/pDMDAAC complex (i.e., in excess of 1:1), as a function of the total SDS/pDMDAAC weight ratio. The systems studied trace counterclockwise along the upper two arcs in Figure 3, with the open symbols referring to the second arc from the top and the closed symbols to the top arc.

determined by analysis of the precipitate for sulfur and nitrogen, respectively. The trend observed in Figure 9 suggests that excess surfactant, as it becomes available beyond 1:1 stoichiometry, associates with the precipitated complex until a ratio of about

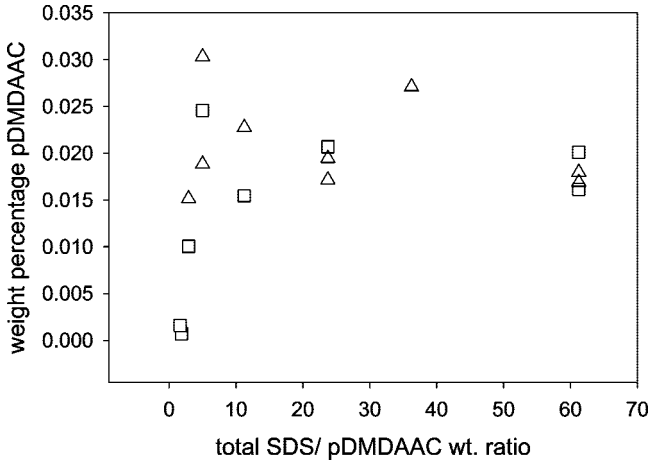

Figure 10. Levels of pDMDAAC in the supernatant phases of the two-phase systems along the upper arc in Figure 3. The weight percentage of polymer is plotted vs the total SDS/pDMDAAC ratio. Different symbols refer to independent trials.

0.2−0.3 mol surfactant/mol of 1:1 complex. Beyond this level of binding, the surfactant apparently enters the supernatant phase, in agreement with the findings of Figure 8. The results from the 1.8% and 4% arcs are indistinguishable within the scatter of the data, suggesting that the level of binding observed is controlled by the stoichiometry of the interaction and not by the bulk levels of the constituents.

As for the pDMDAAC distribution between the precipitated and supernatant phases, it is largely to the precipitate, but the concentration in the supernatant can be determined by Kjeldhal analysis. The results in Figure 10 show that the pDMDAAC level in the supernatant for the 4% pDMDAAC arc is quite low. Across the broad range of surfactant-to-polymer ratio, the soluble polymer level is fairly constant at a level of 0.02 ± 0.005%. SDS is certainly present along with the pDMDAAC in the supernatant, mostly as free micelles or monomers but also in complexation with polymer as soluble species. Unfortunately, the surfactant-to-polymer ratio of these complexes could not be determined directly.

Discussion

Phase Map. The phase map for the present system broadly shows the three expected regions, a two-phase region bordered by isotropic regions for surfactant-rich and polymer-rich compositions. This phase map is in many ways similar to that of the well-studied Polymer JR-400/SDS system, in spite of the lower charge density of the latter polymer. For a comparably high polymer charge density (polystyrene sulfonate), Monteux et al.[25] observed the present trend: isotropic to turbid to macroscopic precipitate to turbid to isotropic with increasing oppositely charged surfactant.

Especially at polymer levels of 0.1% and below, the onset of precipitation from the polymer-rich side with increasing surfactant level occurs close to and roughly parallel with the line of 1:1 stoichiometry. This finding that phase separation commences at approximately constant stoichiometry has also been noted with the Polymer JR-400 system.[69] On moving to the surfactant-rich side of the 1:1 line, the SDS/pDMDAAC system displays asymmetry in that the two-phase area is more stable to excess surfactant than it was to excess polymer. Marques et al.[69] also observed asymmetry in this direction, but the opposite trend has been reported by Svensson et al.[44] where resolubilization on the polymer-rich side required a 100% excess of polymer charge.

The lower left-hand corner of the phase map can be described by saying that the two-phase region narrows and eventually disappears upon dilution in both surfactant and polymer. This disappearance suggests that the stoichiometric complex continues to be relevant and that the complex has a finite strength so that free surfactant and polymer ultimately dominate at high dilution. Zimin et al.[18] observed an isotropic region at high dilution in the SDS/Polymer JR-400 system. At the other extreme, the phase map of the SDS/pDMDAAC system at higher concentration (at or above 1% of either component) is strongly dominated by the two-phase region compared to the Polymer JR-400 system. The higher charge density of pDMDAAC is undoubtedly responsible for this fact. It can be imagined that the high polymer charge density promotes surfactant binding via counterion condensation at very low surfactant levels and that the proximity of the charged groups on the polymer chain also encourages a high cooperativity in the binding. In this regard, the charge spacing in pDMDAAC can be estimated at 0.62 nm,[70] from which the reduced linear charge density ζ can be calculated as 1.2 (ζ is defined as the ratio of the Bjerrum length, 0.71 nm, to the distance between two charged sites on the polymer).[28,29,71,72] Values of ζ in excess of unity are consistent with the counterions condensing on the polymer backbone. The reduced linear charge density for Polymer JR-400 is about 0.36 so that condensation would not be expected. Further, the cooperativity parameter for binding of surfactant to a polymer chain, u, is defined such that $kT \ln u$ is the additional interaction free energy between surfactant molecules bound to neighboring sites.[39] A strong dependence of u on the polymer linear charge density is routinely found. The cooperativity parameter for binding of SDS to pDMDAAC in 1 mM NaCl was measured as 2000 at 298 K by Lee and Moroi,[36] whereas the binding of dodecyl trimethyl ammonium bromide to sodium polyacrylate (whose charge density is similar to pDMDAAC) in the presence of 0.01 M NaBr has been characterized with a cooperativity parameter of 1100.[73] That the two-phase region extends further into surfactant-rich space than is the case with Polymer JR-400 is a sign of the aforementioned resistance to resolubilization by higher charge density polymers like pDMDAAC.

Adsorption. The key conclusion to be drawn from Figures 4 and 5 is that the phase separating from the SDS/pDMDAAC system as the surfactant/polymer ratio is varied can be characterized by a positive surface charge when the polymer is in excess and a negative surface charge when the surfactant is in excess. It likewise appears that adsorption of an SDS/polymer complex is occurring on to glass and that the electrophoretic character of the adsorbed species is largely the same as that of the incipient phase separating out of solution. The depletion studies including Figure 7 support this concept of surfactant/polymer adsorption across a wide range of surfactant-to-polymer ratios. It may seem surprising to find, in the surfactant-rich cases, a net anionic species adsorbing on what would otherwise be a strongly anionic glass surface. However, this observation is quite general[17,55] and at least two possible explanations have been proposed as will be considered further below.

Consideration of these adsorption results reveals some expected and some unexpected findings. That adsorption is detected from the polymer-rich region, where the complex will retain a net cationic charge, is expected in light of the known affinity of pDMDAAC for glass surfaces above their isoelectric point (IEP).[60] The reported adsorption density of 0.8 mg/m^2 is for the pDMDAAC portion of the adsorbing complex. By subtracting the pDMDAAC carbon contribution from the total

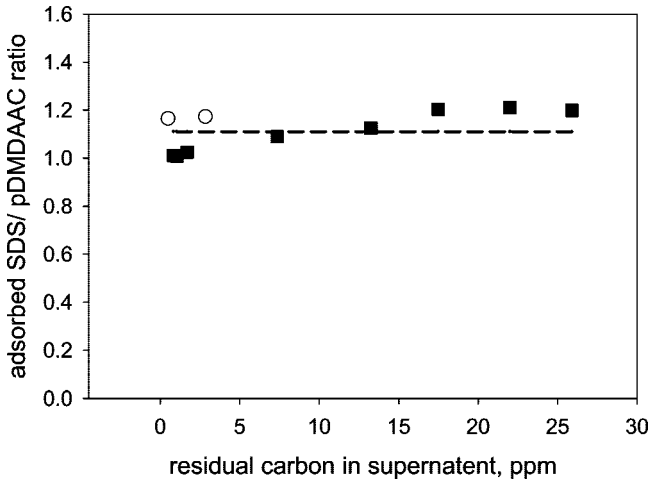

Figure 11. Weight ratio of SDS to pDMDAAC adsorbed on glass powder, as determined by depletion measurements, plotted vs the residual carbon level (data points). The dotted line indicates the ratio in the starting isotropic solution, before addition of glass.

measured carbon depletion, the level of adsorbed SDS can be calculated. Figure 11 is a plot of the SDS/pDMDAAC weight ratio determined in the adsorbed layer as a function of the residual carbon in the supernatant. It can be observed that this ratio is essentially the same as the 1.11 value which characterizes the overall ratio for this particular system. The implication of this finding is that, in the polymer-rich domain, the pDMDAAC adsorbs strongly with all of the available SDS. It seems reasonable, considering as well the electrophoretic results from the incipient precipitates, to extrapolate this finding by proposing that the soluble complexes in the proximity also comprise the vast majority of the available SDS. The measured adsorption density of the pDMDAAC fraction of the adsorbate, 0.8 mg/m^2, is comparable to the 0.35 $\pm$ 0.05 mg/m^2 of pDMDAAC alone previously measured onto controlled-pore glass,[60] once some allowance is made for the SDS content of the complex. In an ion-exchange binding mechanism, the mass of adsorbing polymer should be inversely proportional to its charge density. The charge density of the complex with a 1.1 SDS/pDMDAAC weight ratio is about 40% of that of pDMDAAC alone, meaning that 0.8$-$0.9 mg/m^2 of complex adsorption (expressed in terms of the pDMDAAC component) might have been expected. The adsorption density of the complex considering also the SDS component is found to be about 1.6 mg/m^2. It might also have been expected that some ion exchange would occur upon complex binding, with anionic sites on the glass surface replacing SDS in the complex.[17,55] However, the depletion studies reported above do not suggest significant release of SDS from the complex upon binding.

In the surfactant-rich isotropic system, an adsorption density of 0.3 mg/m^2 was observed for the pDMDAAC portion of the complex. Some SDS will be associated with the adsorbed complex, but the exact levels could not be determined in the isotropic systems. Figure 9 indicates that about 1.25 mol of SDS accompany each mol of DMDAAC in the precipitates found to the surfactant-rich side of 1:1 stoichiometry. Taking this ratio as a lower bounding estimate of the SDS content, the equivalent adsorption density of complex represented in Figure 7c is about 0.80 mg/m^2. Both depletion and electrophoretic mobility data seem to suggest that a net anionic species is adsorbing onto what would otherwise be a strongly anionic glass surface. In rationalizing this surprising finding, an appeal can be made to similar observations by Dedinaite and co-workers,[17,55] where the aforementioned ion exchange was invoked. Entropic arguments can be made to support this mechanism: SDS counterions can be released into solution in exchange for surface anionic sites. A second line of reasoning hinges on the difference between the bulk and localized charge state of the complex[66] and the idea that adsorption is determined by the details of the charge distribution and not the average charge carried by the complex.[74] The binding of SDS beyond 1:1 stoichiometry is currently thought to involve wrapping of the polymer chain around surfactant micelles. The finite flexibility of the polymer chain could limit the matchup of surfactant headgroup and polymer backbone charge so that some polymer sites would retain their original counterions, despite the predominance of surfactant.[21] Then exchange of these original, simple monovalent counterions for surface charge sites could explain the adsorption affinity. Distinguishing between these explanations is not possible from the present limited data.

The irreversibility of adsorption observed in Figure 6 is not unexpected, as noted previously. The translational entropy gain upon replacement of the surface counterions by the surfactant/polymer complex increases upon dilution. The alteration of the adsorbate upon dilution along the SDS-rich phase boundary is more noteworthy and suggests that the 1:1 stoichiometric complex is especially resistant to dilution, though the same cannot be said about the surfactant bound beyond stoichiometry. This observation is in keeping with the (ir)reversibility of the phase behavior, in which surfactant-rich systems could be suitably diluted with polymer to yield the rubbery 1:1 precipitate, but that species could then not be further modified.

The experimental adsorption data for the polymer-rich species can be used to relate the adsorption density to the glass particle ζ-potential. With the identification of the charge nature of the adsorbed species, it is possible to check the results for self-consistency in terms of the Gouy$-$Chapman model for the diffuse double layer around the glass particles. The surface charge density σ of the particles can be expressed in terms of the ζ-potential ζ as[75]

$$\sigma \approx (2\kappa\varepsilon_0\varepsilon_r kT/ze)\ \sinh\{ze\zeta/2kT\} \qquad (2)$$

where all other symbols have been defined previously.

For a symmetric 1:1 electrolyte in water at 25 °C, this expression simplifies to[64]

$$\sigma \approx 11.74\sqrt{c}\ \sinh\{19.46z\zeta\} \qquad (3)$$

where σ is in μC/cm^2, ζ is expressed in volts, and the electrolyte concentration c is in moles per liter. The level of adsorption measured on the polymer-rich side is shown in Figure 7a to correspond to 0.06$-$0.07 mg of nitrogen/m^2. In the absence of any counterions, the adsorbed DMDAAC units would contribute a surface charge of 41$-$48 μC/cm^2. However, Figure 7b indicates that there are approximately 0.56 SDS ions present for each DMDAAC unit in the adsorbate so that a net surface charge of about 18$-$21 μC/cm^2 would be predicted. In addition, the underlying surface charge of the glass surface must also be accounted for. The measured ζ-potential of the glass surface prior to any adsorption is in the range of $-$60 to $-$65 mV, which translates via eq 3 to a surface charge of about $-$1.8 μC/cm^2. The net surface charge would thus be predicted to lie in the range of 16$-$19 μC/cm^2. In comparison, the ζ-potential for the glass particles after adsorption is reported in Figure 5 to be about +20 mV, meaning that the surface has an apparent surface charge of only 0.5 μC/cm^2, about 3% of that expected from the measured adsorption. Part of this discrepancy can be attributed to the uncertainties in the location of the plane of shear in the

case of adsorbed layers. However, the overriding conclusion is that a significant fraction of the chloride counterions are associated with the adsorbed layer, reducing its net charge. A similarly high degree of counterion binding has been observed by Zimmermann et al.[76] for poly(acrylic acid) brushes at pH 9. In that case, ζ-potential measurements indicated that only 1% of the polymer charge was uncompensated. The degree of counterion binding found with a complex involving pDMDAAC is more profound than that which would be encountered with a lower charge density polymer such as Polymer JR.[8]

Composition of Separated Phases and Implications for Resolubilization. For a broad range of total surfactant-to-polymer ratio, corresponding to the sections of the 1.8% and 4% pDMDAAC arcs between 1:1 stoichiometry and the surfactant-rich phase boundary, the precipitated phase consists of 1.2−1.3 mol of SDS/mol of polymer repeat unit. This composition can be interpreted as 0.2−0.3 mol of SDS associated/mol of 1:1 surfactant/polymer complex. This limited level of excess binding is significantly below 1 mol surfactant/mol complex, eliminating the possibility of a full excess surfactant layer binding beyond stoichiometry. It is noteworthy that the 0.2−0.3 mol excess species appears to be significant over more than an order-of-magnitude of surfactant/polymer ratio (Figure 9), covering the formulation space typical of most applications for this technology. Across the same range of surfactant-to-polymer ratio, the precipitated phase is in equilibrium with a supernatant containing a soluble complex whose polymer concentration is fairly constant at 0.02% (Figure 10).

These results can also be used to make some relevant observations concerning resolubilization of the surfactant/polymer complex precipitate. At the highest total surfactant/polymer ratios considered in Figures 9 and 10, the polymer concentration corresponding to the isotropic transition is still almost an order-of-magnitude away (i.e., the transition occurs to still higher total ratios). Yet the ratio of SDS to polymer *in the complex precipitate* reported in Figure 9 does not suggest an increasing trend in this ratio with increasing total ratio. Nor does the level of the soluble complex, as indicated by the polymer solubility, appear to change as resolubilization is approached. Although most of the prior resolubilization studies have involved increasing the surfactant concentration at constant polymer level, the route taken along the arcs in Figure 3 (to the surfactant-rich side of 1:1 stoichiometry) is clearly one of decreasing the polymer concentration at essentially constant surfactant concentration. In this context, the results of Figure 10 may be relevant. The solubility of the polymer species, presumably complexed with surfactant, has been noted above to be in the vicinity of 0.02% along a path which corresponds to the upper-most arc of Figure 3. As the total polymer content is decreased along this arc, a transition to an isotropic phase occurs at about 0.01% polymer. The proximity of the solubility with the phase boundary suggests that resolubilization can be achieved by diluting the total polymer level until it reaches its solubility limit. This view of resolubilization, based on the level of soluble polymer being the same on either side of the phase boundary, does not make any requirements of the precipitate other than that its mass must decrease upon dilution up to the solubility boundary. However, a precipitate of constant composition in equilibrium with a soluble complex of constant polymer concentration can be interpreted simply, though not uniquely, in terms of the same SDS/pDMDAAC complex. This complex would be the 0.25 mol ratio excess species, composing the precipitate phase and being sparingly soluble in the supernatant. When diluting the surfactant/polymer complex precipitate at essentially constant surfactant level along the arcs of Figure 3, the solubility limit of the complex is eventually reached and the system becomes isotropic, without necessitating a change in the composition of the complex.

Conclusions

(i) The glass powder particles used in this study have a p.z.c. of 3.0 ± 0.5 in 0.01 M NaCl. Thus these particles will be negatively charged when dispersed in the surfactant/polymer mixture.

(ii) The phase map for the system SDS/pDMDAAC shows, at 0.01 M NaCl, behavior typical of surfactant/oppositely charged polyelectrolyte mixtures.

(iii) A two-phase region in the phase map lies asymmetrically around the 1:1 stoichiometry of surfactant charge groups to polymer charge units. To the polymer-rich side of 1:1 stoichiometry, any surfactant/polymer complex is soluble so that phase separation is driven by charge compensation. On the surfactant-rich side, the two-phase region persists to great excess of surfactant. However, the overall controlling principle is still charge compensation.

(iv) Most applications of surfactant/polymer technology occur at compositions which lie well within the two-phase region but to the surfactant-rich side of 1:1 stoichiometry.

(v) The phase separating from the SDS/pDMDAAC blend as the SDS/polymer ratio is varied is characterized by a positive surface charge when the polymer is in excess and a negative surface charge when the SDS is in excess.

(vi) The surface charge properties of the precipitated phases are essentially identical to those of glass particles dispersed in the adjacent isotropic position in the phase map. Depletion studies find that the soluble complexes adsorb onto the glass surface without change in the complex composition. Thus, the surfactant/polymer complex which forms in the bulk is the same as that adsorbing onto the particle. This observation holds in the polymer-rich isotropic region and also in the surfactant-rich isotropic region—where the glass surface and the complex have the same net surface charge. A high-affinity isotherm characterizes both regions, with a plateau coverage of about 0.8 mg polymer/m^2 on the polymer-rich and 0.3 mg polymer/m^2 on the surfactant-rich sides.

(vii) Once adsorbed, these complexes are not readily removed by rinsing. Extensive dilution of adsorbed surfactant-rich complexes releases the excess SDS, tending to make the particles more hydrophobic.

(viii) Chemical analysis reveals that the surfactant/polymer precipitates in the extensive surfactant-rich portion of the two-phase region can be represented as a 1:1 charge complex with an additional 0.2−0.3 mol of SDS/mol of complex. Resolubilization of this species is argued to correspond to dilution at constant surfactant level until the solubility limit of the complex is achieved.

Acknowledgment. It is a pleasure to thank Dr. Shanling Shi for providing the electron micrograph in Figure 1. Enlightening discussions with Unilever colleagues K. P. Ananthapadmanabhan and A. Lips and with Dr. Brian Pethica of Princeton University are gratefully acknowledged. We also thank Unilever Research and Development for allowing us to publish this work.

References and Notes

(1) Robb, I. D. In *Anionic Surfactants*; Surfactant Science Series Vol. *11*; Lucassen-Reynders, E., Ed.; Marcel Dekker: New York, 1981.

(2) Saito, S. In *Nonionic Surfactants*; Schick, M. J., Ed.; Marcel Dekker: New York, 1991.

(3) Hayakawa, K.; Kwak, J. C. T. In *Cationic Surfactants*, 2nd ed.; Rubingh, D. N., Holland, P. M., Eds; Marcel Dekker: New York, 1991.
(4) Goddard, E. D. In *Interactions of Surfactants with Polymers and Proteins*; Goddard, E. D., Ananthapadmanabhan, K. P., Eds.; CRC Press: New York, 1993.
(5) Kwak, J. C. T. In *Polymer−Surfactant Systems*; Kwak, J. C. T., Ed.; Surface Science Series, Vol. *77*; Marcel Dekker: New York, 1998.
(6) Goddard, E. D. *J. Colloid Interface Sci.* **2002**, *256*, 228.
(7) Miyake, M.; Kakizawa, Y. *Colloid Polym. Sci.* **2002**, *280*, 18.
(8) Terada, E.; Samoshina, Y.; Nylander, T.; Lindman, B. *Langmuir* **2004**, *20*, 1753.
(9) Goddard, E. D.; Hannan, R. B. *J. Am. Oil Chem. Soc.* **1977**, *54*, 561.
(10) Qian, L.; Charlot, M.; Perez, E.; Luengo, G.; Potter, A.; Cazeneuve, C. *J. Phys. Chem. B* **2004**, *108*, 18608.
(11) Pagac, E. S.; Prieve, D. C.; Tilton, R. D. *Langmuir* **1998**, *14*, 2333.
(12) Chen, W.-J. *J. Chin. Inst. Chem. Eng.* **2001**, *32*, 95.
(13) Cabane, B.; Lindell, K.; Engstrom, S.; Lindman, B. *Macromolecules* **1996**, *29*, 3188.
(14) Goddard, E. D.; Hannan, R. B. *J. Colloid Interface Sci.* **1976**, *55*, 73.
(15) Goddard, E. D.; Hannan, R. B.; Matteson, G. H. *J. Colloid Interface Sci.* **1977**, *60*, 214.
(16) Anthony, O.; Marques, C. M.; Richetti, P. *Langmuir* **1998**, *14*, 6086.
(17) Dedinaite, A.; Claesson, P. M. *Langmuir* **2000**, *16*, 1951.
(18) Zimin, D.; Craig, V. S. J.; Kunz, W. *Langmuir* **2004**, *20*, 2282.
(19) Zhou, S.; Xu, C.; Wang, J.; Golas, P.; Batteas, J. *Langmuir* **2004**, *20*, 8482.
(20) Goldraich, M.; Schwartz, J. R.; Burns, J. L.; Talmon, Y. *Colloids Surf., A* **1997**, *125*, 231.
(21) Wang, Y.; Kimura, K.; Dubin, P. L.; Jaeger, W. *Macromolecules* **2000**, *33*, 3324.
(22) Merta, J.; Torkkeli, M.; Ikonen, T.; Serimaa, R.; Stenius, P. *Macromolecules* **2001**, *34*, 2937.
(23) Proietti, N.; Amato, M. E.; Masci, G.; Segre, A. L. *Macromolecules* **2002**, *35*, 4365.
(24) Wesley, R. D.; Cosgrove, T.; Thompson, L.; Armes, S. P.; Baines, F. L. *Langmuir* **2002**, *18*, 5704.
(25) Monteux, C.; Williams, C. E.; Meunier, J.; Anthony, O.; Bergeron, V. *Langmuir* **2004**, *20*, 57.
(26) Ranganathan, S.; Kwak, J. C. T. *Langmuir* **1996**, *12*, 1381.
(27) Bai, G.; Santos, L.M.N.B.F.; Nichifor, M.; Lopes, A.; Bastos, M. *J. Phys. Chem. B* **2004**, *108*, 405.
(28) Wang, C.; Tam, K. C. *Langmuir* **2002**, *18*, 6484.
(29) Wang, C.; Tam, K. C. *J. Phys. Chem. B* **2004**, *108*, 8976.
(30) Berret, J.-F. *J. Chem. Phys.* **2005**, *123*, 164703.
(31) Chakraborty, T.; Charkraborty, I.; Ghosh, S. *Langmuir* **2006**, *22*, 9905.
(32) Wang, H.; Wang, Y.; Yan, H.; Zhang, J.; Thomas, R. K. *Langmuir* **2006**, *22*, 1526.
(33) Babak, V. G.; Merkovich, E. A.; Desbrieres, J.; Rinaudo, M. *Polym. Bull.* **2000**, *45*, 77.
(34) Kasseh, M.; Keh, E. *Colloid Polym. Sci.* **2006**, *284*, 489.
(35) Lapitsky, Y.; Parikh, M.; Kaler, E. W. *J. Phys. Chem. B* **2007**, *111*, 8379.
(36) Lee, J.; Moroi, Y. *Bull. Chem. Soc. Jpn.* **2003**, *76*, 2099.
(37) Lee, J.; Moroi, Y. *J. Colloid Interface Sci.* **2004**, *273*, 645.
(38) Mukerjee, P.; Mysels, K. J. *Critical Micelle Concentrations of Aqueous Surfactant Systems*; National Standards Reference Data Series *36*; National Bureau of Standards: Washington, DC, 1971.
(39) Hansson, P.; Almgren, M. *J. Phys. Chem.* **1996**, *100*, 9038.
(40) Zheng, X.; Cao, W. *Eur. Polym. J.* **2001**, *37*, 2259.
(41) Jain, N.; Trabelsi, S.; Guillot, S.; McLoughlin, D.; Langevin, D.; Letellier, P.; Turmine, M. *Langmuir* **2004**, *20*, 8496.
(42) Guillot, S.; McLoughlin, D.; Jain, N.; Delsanti, M.; Langevin, D. *J. Phys.: Condens. Matter* **2003**, *15*, S219.
(43) Ilekti, P.; Martin, T.; Cabane, B.; Piculell, L. *J. Phys. Chem. B* **1999**, *103*, 9831.
(44) Svensson, A.; Sjostrom, J.; Scheel, T.; Piculell, L. *Colloids Surf., A* **2003**, *228*, 91.
(45) Deo, P.; Deo, N.; Somasundaran, P.; Moscatelli, A.; Jockusch, S.; Turro, N. J.; Ananthapadmanabhan, K. P.; Ottaviani, M. F. *Langmuir* **2007**, *23*, 5906.
(46) Bai, G.; Nichifor, M.; Lopes, A.; Bastos, M. *J. Phys. Chem. B* **2005**, *109*, 518.
(47) Friman, R.; Backlund, S.; Hassan, O.; Alfredsson, V.; Linden, M. *Colloids Surf., A* **2006**, *291*, 148.
(48) Svensson, A.; Piculell, L.; Cabane, B.; Ilekti, P. *J. Phys. Chem. B* **2002**, *106*, 1013.
(49) Shubin, V. *Langmuir* **1994**, *10*, 1093.
(50) Ninness, B. J.; Bousfield, D. W.; Tripp, C. P. *Colloids Surf., A* **2002**, *203*, 21.
(51) McNamee, C. E.; Matsumoto, M.; Hartley, P. G.; Mulvaney, P.; Tsujii, Y.; Nakahara, M. *Langmuir* **2001**, *17*, 6220.
(52) Penfold, J.; Tucker, I.; Staples, E.; Thomas, R. K. *Langmuir* **2004**, *20*, 7177.
(53) Li, H.; Tripp, C. P. *Langmuir* **2004**, *20*, 10526.
(54) Arnold, G. B.; Breuer, M. M. *Colloids Surf.* **1985**, *13*, 103.
(55) Dedinaite, A.; Claesson, P. M.; Bergstrom, M. *Langmuir* **2000**, *16*, 5257.
(56) Ilekti, P.; Piculell, L.; Tournilhac, F.; Cabane, B. *J. Phys. Chem. B* **1998**, *102*, 344.
(57) Terada, E.; Samoshina, Y.; Nylander, T.; Lindman, B. *Langmuir* **2004**, *20*, 6692.
(58) Li, Y.; Xia, J.; Dubin, P. L. *Macromolecules* **1994**, *27*, 7049.
(59) Rigsbee, D. R.; Dubin, P. L. *Langmuir* **1996**, *12*, 1928.
(60) Tartakovsky, A.; Drutis, D. M.; Carnali, J. O. *J. Colloid Interface Sci.* **2003**, *263*, 408.
(61) Poptoshev, E.; Rutland, M. W.; Claesson, P. M. *Langmuir* **2000**, *16*, 1987.
(62) Laughlin, R. G. *The Aqueous Phase Behavior of Surfactants*; Academic Press: London, 1996.
(63) Myers, D. *Surfaces, Interfaces, and Colloids, Principles and Applications*; Wiley: New York, 1999.
(64) Hunter, R. J. *Foundations of Colloid Science*, 2nd ed.; Oxford University Press: Oxford, 2001.
(65) Pashley, R. M.; Karaman, M. E. *Applied Colloid and Surface Chemistry*; Wiley: Chichester, England, 2004.
(66) Buchhammer, H.-M.; Petzold, G.; Lunkwitz, K. *Langmuir* **1999**, *15*, 4306.
(67) Liu, J.; Vandenberghe, J.; Masliyah, J.; Xu, Z.; Yordan, J. *Miner. Eng.* **2007**, *20*, 566.
(68) Kharas, G. B.; Heiskell, J. R.; Herrman, J.; Kasudia, P. T.; Schreiber, P. J.; Passe, L. B.; Bravo-Grimaldo, E.; Bazuin, C. G.; Romanowski, P. T.; Schueller, R. M. *J. Macromol. Sci., Pure Appl. Chem.* **2006**, *43*, 213.
(69) Marques, E. F.; Regev, O.; Khan, A.; da Graca Miguel, M.; Lindman, B. *Macromolecules* **1999**, *32*, 6626.
(70) Kayitmazer, A. B.; Shaw, D.; Dubin, P. L. *Macromolecules* **2005**, *38*, 5198.
(71) Manning, G. S. *J. Chem. Phys.* **1969**, *51*, 924.
(72) Hodgson, D. F.; Amis, E. J. In *Polyelectrolytes: Science and Technology*; Hara, M., Ed.; Marcel Dekker: New York, 1992.
(73) Linse, P.; Piculell, L.; Hansson, P. In *Polymer Surfactant Systems*; Kwak, J. C. T., Ed.; Surfactant Science Series Vol. *77*; Marcel Dekker: New York, 1998.
(74) Kamiyama, Y.; Israelachvili, J. *Macromolecules* **1992**, *25*, 5081.
(75) Verwey, E. J.; Overbeek, J. Th. G. *Theory of the Stability of Lyophobic Colloids*; Dover: New York, 1948.
(76) Zimmermann, R.; Norde, W.; Cohen Stuart, M. A.; Werner, C. *Langmuir* **2005**, *21*, 5108.

JP801079V